Published online 13 May 2017

Nucleic Acids Research, 2017, Vol. 45, No. 12 ***7507–7514***
doi: 10.1093/nar/gkx413

Madumycin II inhibits peptide bond formation by forcing the peptidyl transferase center into an inactive state

Ilya A. Osterman[1,2], Nelli F. Khabibullina[3], Ekaterina S. Komarova[4], Pavel Kasatsky[5], Victor G. Kartsev[6], Alexey A. Bogdanov[1], Olga A. Dontsova[1,2], Andrey L. Konevega[5,7,*], Petr V. Sergiev[1,2,*] and Yury S. Polikanov[3,8,*]

[1]Lomonosov Moscow State University, Department of Chemistry and A.N. Belozersky Institute of Physico-Chemical Biology, Moscow 119992, Russia, [2]Skolkovo Institute of Science and Technology, Skolkovo, Moscow region 143025, Russia, [3]Department of Biological Sciences, University of Illinois at Chicago, Chicago, IL 60607, USA, [4]Lomonosov Moscow State University, Department of Bioengineering and Bioinformatics, Moscow 119992, Russia, [5]Petersburg Nuclear Physics Institute, NRC "Kurchatov Institute", Gatchina 188300, Russia, [6]Interbioscreen Ltd, Chernogolovka, Moscow Region 142432, Russia, [7]Peter the Great St.Petersburg Polytechnic University, Saint Petersburg, 195251, Russia and [8]Department of Medicinal Chemistry and Pharmacognosy, University of Illinois at Chicago, Chicago, IL 60607, USA

Received February 15, 2017; Revised April 26, 2017; Editorial Decision April 27, 2017; Accepted May 04, 2017

ABSTRACT

The emergence of multi-drug resistant bacteria is limiting the effectiveness of commonly used antibiotics, which spurs a renewed interest in revisiting older and poorly studied drugs. Streptogramins A is a class of protein synthesis inhibitors that target the peptidyl transferase center (PTC) on the large subunit of the ribosome. In this work, we have revealed the mode of action of the PTC inhibitor madumycin II, an alanine-containing streptogramin A antibiotic, in the context of a functional 70S ribosome containing tRNA substrates. Madumycin II inhibits the ribosome prior to the first cycle of peptide bond formation. It allows binding of the tRNAs to the ribosomal A and P sites, but prevents correct positioning of their CCA-ends into the PTC thus making peptide bond formation impossible. We also revealed a previously unseen drug-induced rearrangement of nucleotides U2506 and U2585 of the 23S rRNA resulting in the formation of the U2506•G2583 wobble pair that was attributed to a catalytically inactive state of the PTC. The structural and biochemical data reported here expand our knowledge on the fundamental mechanisms by which peptidyl transferase inhibitors modulate the catalytic activity of the ribosome.

INTRODUCTION

Understanding the structural basis for the action of antibiotics is paramount for the development of better antimicrobials and instrumental to elucidating the mechanisms of cellular processes. Protein biosynthesis is one of the major targets for a large set of antibiotics that belong to diverse structural classes and act upon various steps of translation (1). Streptogramins are macrocyclic antibiotics divided into A and B subclasses that bind to adjacent sites within the peptide exit tunnel in the large subunit of the ribosome (2). There are several drugs among streptogramins that are approved for clinical use, such as Synercid, a mixture of type A streptogramin dalfopristin and type B streptogramin quinupristin (3).

Structures of several type A streptogramins in complexes with the large ribosomal subunit from the archaeon *Haloarcula marismortui* (4), or bacterium *Deinococcus radiodurans* (5), and in complex with the 70S ribosome from *Escherichia coli* (3) have been reported previously. However, despite the importance of the aforementioned structures, neither of them contained mRNA and tRNAs and, therefore, did not represent a functional state of the ribosome. Given the proximity of the streptogramin binding sites to the location of the tRNA-substrates in the PTC, the actual mechanism of inhibition could be studied structurally using functional complexes of the bacterial ribosome.

Based on biochemical and structural studies, we present the mechanism by which the simplest type A

*To whom correspondence should be addressed. Tel: +1 312 413 2408; Fax: +1 312 431 2691; Email: yuryp@uic.edu
Correspondence may also be addressed to Andrey L. Konevega. Tel: +7 813 714 6093; Fax: +7 813 713 2303; Email: konevega_al@pnpi.nrcki.ru
Correspondence may also be addressed to Petr V. Sergiev. Tel: +7 495 939 5418; Fax: +7 495 939 3181; Email: petya@genebee.msu.ru

streptogramin—madumycin II (MADU)—inhibits protein synthesis. One structural variation between MADU and other type A streptogramins is that it contains an alanine residue instead of proline (Figure 1A) (6,7). We demonstrate that MADU stalls the ribosome at the start codon with the initiator fMet-tRNA^{fMet} bound to the P site and inhibits the formation of the first peptide bond. Our structural data show that the binding of MADU into the PTC leads to significant structural re-arrangements of several key nucleotides around the PTC. Additionally, it causes a flip of the A76 of the P-site tRNA and prevents the full accommodation of the A-site tRNA making peptide bond formation unlikely.

MATERIALS AND METHODS

Materials for biochemical experiments

Madumycin II was provided by Victor G. Kartsev from Interbioscreen Ltd.

In vitro translation analysis

The inhibition of firefly luciferase synthesis by MADU was assessed essentially as described previously (8). Briefly, the *in vitro* transcribed firefly luciferase mRNA was translated in the *E. coli* S30 cell-free system prepared according to (9). Reactions programmed with 200 ng mRNA were carried out in 5 μl aliquots at 37°C for 30 min and the activity of *in vitro* synthesized luciferase was assessed using 5 μl of substrate from the Steady-Glo® Luciferase Assay System (Promega).

Peptide formation assays

The inhibition of the peptidyl transferase reaction by MADU was monitored by fMet-Phe dipeptide, fMet-Phe-Puromycin and fMet-Val-Phe tripeptide formation assays. *Escherichia coli* 70S ribosome initiation complexes programmed with MFTI-encoding mRNA and containing initiator fMet-tRNA^{fMet} in the P site were mixed with various amounts of MADU (dissolved in DMSO) and pre-formed ternary complex [^{14}C]-Phe-tRNA^{Phe}•EF-Tu•GTP in buffer containing 50 mM Tris-HCl (pH 7.5), 70 mM NH_4Cl, 30 mM KCl, 7 mM $MgCl_2$ (10). After incubation at 37°C for different time intervals the reaction was terminated by addition of 0.5 M KOH, which also hydrolyzed amino acids or dipeptide/tripeptide moieties from the carrying tRNA molecules by alkaline hydrolysis (30 min at 37°C). Free unincorporated amino acids were separated from di- and tripeptides by the reverse-phase HPLC chromatography (11) and the amounts of radioactively labeled [^{14}C]-Phe or [^{14}C]-Val incorporated into the peptides were measured using scintillation counter (Beckman LS6500).

Toe-printing analysis

The position of the ribosome on the mRNA was monitored using a toe-printing assay that was carried out essentially as previously described (12) using *osmC* mRNA or its mutant forms containing insertions of either GGC (glycine) or AUC (isoleucine) codon after the initiator AUG codon as a templates for protein translation (13).

Crystallographic structure determination

Ribosome complexes with mRNA and tRNAs were formed by mixing 5 μM *Thermus thermophilus* 70S ribosomes with 10 μM mRNA and incubation at 55°C for 10 min, followed by addition of 20 μM P-site (fMet-tRNA$_i^{fMet}$) and 20 μM A-site (Phe-tRNA^{Phe}) substrates (14,15). Each of the last two steps was allowed to reach equilibrium for 10 min at 37°C. For co-crystallization of MADU with the ribosome, the antibiotic was added to a final concentration of 200 μM, and the complex was left at room temperature for an additional 15 min prior to crystallization. All *Tth* 70S ribosome complexes were formed in the buffer containing 5 mM HEPES–KOH (pH 7.6), 50 mM KCl, 10 mM NH_4Cl, and 10 mM $Mg(CH3COO)_2$, and then crystallized in the buffer containing 100 mM Tris–HCl (pH 7.6), 2.9% (w/v) PEG-20K, 7–12% (v/v) MPD, 100–200 mM arginine, 0.5 mM β-mercaptoethanol (16). Crystals were grown by the vapor diffusion method in sitting drops at 19°C and stabilized as described previously (8,14,15) with 100 μM MADU included in the cryo-protection buffers. Diffraction data were collected using beamline 24ID-C at the Advanced Photon Source. All crystals belonged to the primitive orthorhombic space group $P2_12_12_1$ with approximate unit cell dimensions of 210 Å × 450 Å × 620 Å and contained two copies of the 70S ribosome per asymmetric unit. Each structure was solved by molecular replacement using PHASER from the CCP4 program suite (17). The search model was generated from the previously published structure of *T. thermophilus* 70S ribosome with bound mRNA and tRNAs (PDB entry 4Y4P from (15)). The initial molecular replacement solutions were refined by rigid body refinement with the ribosome split into multiple domains, followed by positional and individual B-factor refinement. The final models of the 70S ribosome in complex with MADU and mRNA/tRNAs was generated by multiple rounds of model building in COOT (18), followed by refinement in PHENIX (19). The statistics of data collection and refinement are compiled in Supplementary Table S1.

RESULTS AND DISCUSSION

MADU inhibits protein synthesis by targeting the ribosome

MADU belongs to type A streptogramins, a known class of efficient inhibitors of protein synthesis. The effects of MADU (Figure 1A) have not been studied before and this study seeks to provide a detailed report on structure–function relationship not only for this particular compound, but for the whole class in general. First, we tested the ability of MADU to inhibit protein synthesis *in vitro* using an *E. coli* S30 extract translation system supplemented with the firefly luciferase mRNA. We observed a dose-dependent inhibition of translation by MADU with an $IC_{50} = 0.3 \pm 0.03$ μM. At 5 μM concentration, MADU reduced the efficiency of protein synthesis by >100-fold (Figure 1B), revealing its strong inhibitory properties.

An antibiotic can hinder protein synthesis by interference with the activity of the ribosome or any of the various factors and enzymes that are involved in protein production. It has been reported previously that the antibiotic virginiamycin M (type A streptogramin) specifically inhibits

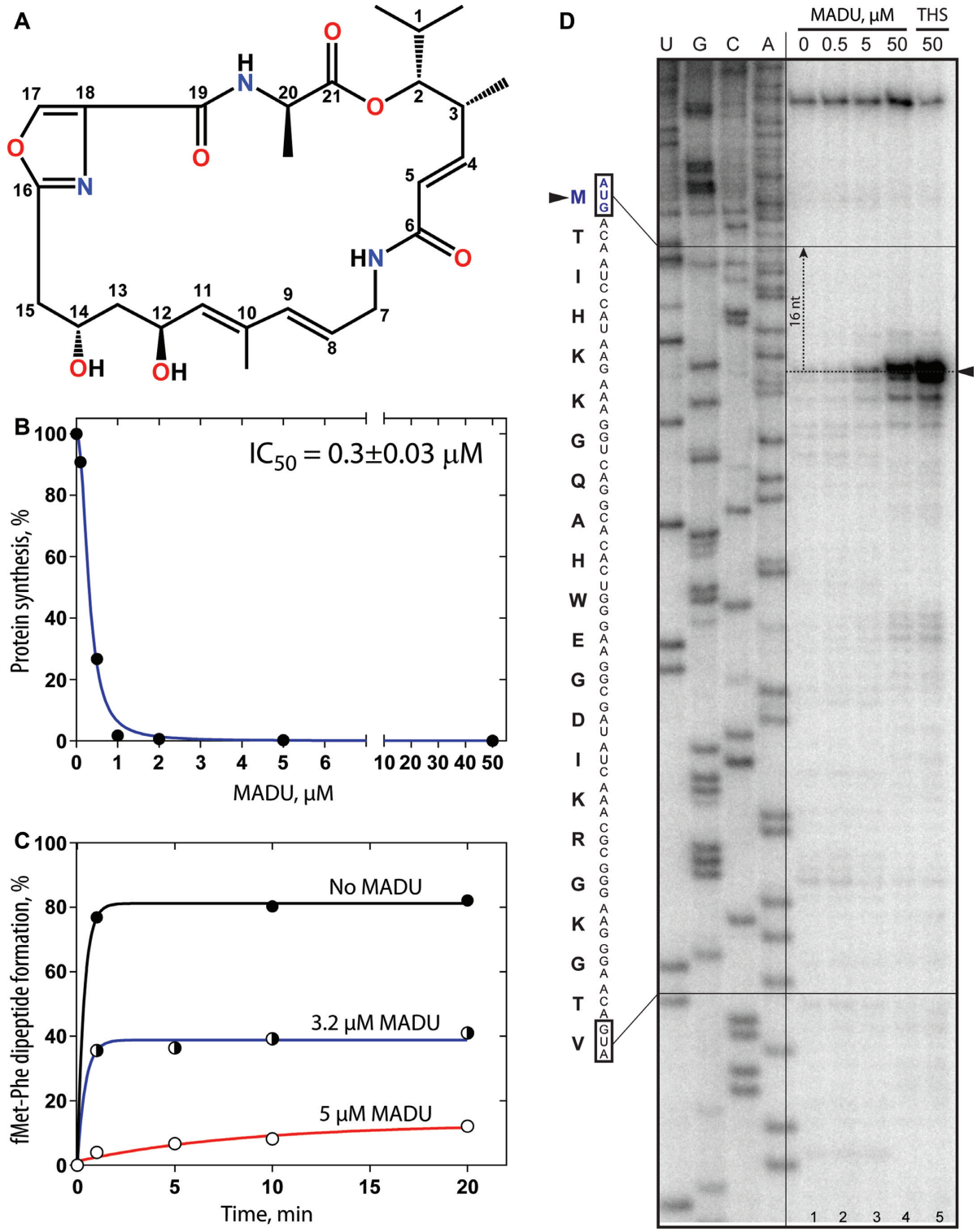

Figure 1. Inhibition of protein synthesis *in vitro* by MADU and its chemical structure. (**A**) Chemical structure of madumycin II. (**B**) Inhibition of protein synthesis by increasing concentrations of MADU in the *in vitro* cell-free transcription-translation coupled system. Shown is the relative enzymatic activity of *in vitro* synthesized firefly luciferase. (**C**) Inhibition of fMet-Phe dipeptide formation by increasing concentrations of MADU. Shown are the relative yields of dipeptide formed in the absence of MADU (filled circles), or in the presence of 3.2 μM (semi-filled circles), or 5 μM (open circles) MADU as a function of time. (**D**) Ribosome stalling by MADU on the *osmC* mRNA as revealed by reverse transcription inhibition (toe-printing) in a recombinant (PURExpress) cell free translation system. U, G, C, A correspond to sequencing lanes for the *osmC* mRNA. Lanes 1–4 correspond to the toe-printing of ribosomes stalled in the absence of inhibitor (0) or in the presence of increasing concentrations of MADU (0.5, 5 and 50 μM) or the positive control antibiotic thiostrepton (THS, 50 μM). Sequence of the *osmC* mRNA together with the corresponding amino acid sequence of the translated product are shown on the left. Stalling of ribosomes at the AUG start codon is shown by the black triangles. Vertical dashed arrow indicates that there is a 16-nt difference between the position, at which reverse transcriptase terminates, and the actual mRNA-codon in the P site of the ribosome.

the peptidyl transferase reaction in a polyU-guided *in vitro* translation system (20). To investigate whether MADU can inhibit peptide bond formation during translation of natural mRNAs, we measured the accumulation of the fMet-Phe dipeptide after mixing of the initiation 70S ribosome complex containing initiator fMet-$tRNA_i^{fMet}$ with the Phe-$tRNA^{Phe}$•EF-Tu•GTP ternary complex. The addition of MADU to a concentration of 5 μM caused nearly 5-fold reduction of the dipeptide formation, corroborating earlier findings (Figure 1C). Although these results point to the ribosome as the likely target for the action of MADU, it remains unclear as to which step of translation is inhibited.

To determine the exact step of translation that is inhibited by MADU, a primer extension inhibition (toe-printing) assay was employed (21). This method allows unambiguous identification of the drug-induced ribosome stalling site along the mRNA with single nucleotide precision (13). It also allows to infer whether the tRNAs are bound to the ribosome or not in the presence of a drug. Similarly to pristinamycin IIB (type A streptogramin antibiotic that was assessed previously by toe-printing (13)), addition of MADU to the PURExpress cell-free transcription-translation system programmed with the *osmC* mRNA results in a dose-dependent ribosome stalling at the start codon (Figure 1D, lanes 5–8). Thiostrepton is used as a positive control that is known to stall ribosomes at the first codon (Figure 1D, lane 9). This result indicates that MADU does not interfere with the formation of the initiation complex that contains at least one tRNA in the P site. However, the formation of the first peptide bond and progression of the ribosome to the next codon is suppressed by this drug, at least in the case of the *osmC* mRNA. To further characterize the mechanism of ribosome inhibition by MADU, the compound was bound to a functional ribosome complex containing mRNA and tRNAs, crystallized and its structure was determined.

MADU allows binding but prevents proper positioning of both A- and P-tRNAs

To determine the mode of binding of MADU in the context of the ribosome functional complex, we crystallized *Thermus thermophilus* (*Tth*) 70S ribosomes in the presence of MADU, mRNA and deacylated A-, P-, and E-site tRNAs and determined the structure of the obtained complex by X-ray crystallography at 2.8 Å resolution. The unbiased difference Fourier map revealed positive electron density similar in shape to the chemical structure of MADU (Figure 2A). A single binding site for MADU was observed in the peptidyl transferase center of the large ribosomal subunit spanning both A and P sites (Figure 2B). In ribosome complex with mRNA and tRNAs, the binding site of MADU is very similar to the binding sites of virginiamycin M, dalfopristin, or flopristin (all proline-containing type A streptogramin antibiotics), which were observed previously on a vacant *E. coli* ribosome in the absence of mRNA and tRNAs (Supplementary Figure S1) (3).

In our complex, the electron density corresponding to the CCA-end of the A-site tRNA is not visible, while the rest of the A-site tRNA is present, suggesting a significant MADU-dependent flexibility in that region. This flexibility is likely to arise from the lack of proper coordination of the CCA-end with the ribosome. The extent of inhibition by MADU might, therefore, depend on the size of the side chain of the amino acid attached to the A-tRNA. To check this hypothesis, we repeated toe-printing experiments with either isoleucine (bulky side chain) or glycine (no side chain) as the second amino acid encoded by the mRNA (Supplementary Figure S2). While we can see noticeably more ribosomes progressing to the second codon in the case of glycine as compared with the isoleucine, a significant fraction of the ribosomes is stalled at the start codon regardless of the second triplet. In agreement with this result is the observation that the binding site of MADU significantly overlaps with the normal location of the entire amino-acyl moiety of the A-site substrate, as well as with the formyl-methionine moiety and A76 residue of the P-site substrate (Figures 2C, D and 3A, B). Importantly, based on the structure MADU collides not only with the side chain of the amino acid in the A site, but also with the main-chain atoms, suggesting that accommodation of even the smallest amino acids, such as glycine, would be problematic.

The most dramatic effect of MADU binding is observed for nucleotide A76 of the P-site tRNA, which flips out by 180° from its normal location towards the interface between the two subunits. In line with our findings, flipping of the 3′-terminal residue of the P-site bound tRNA was proposed previously on the basis of cross-linking data (22) but has not yet been confirmed structurally. Interestingly, a very similar flipped-out conformation of the deacylated nucleotide A76 has been observed recently in the absence of any drugs around the PTC (23). Although, the P-site tRNA is deacylated in our structure, *in silico* modelling shows that presence of the formyl-methionine group attached to adenine 76 is compatible with the structure and would not cause any collision (Supplementary Figure S3). Therefore, we propose a model in which nucleotide A76 of the P-site tRNA can oscillate between the two conformations: the flipped out non-productive state and properly positioned reactive state. In our model, the flipped out conformation could be stabilized by the presence of the drug, such as MADU, or by the deacylation of the P-site tRNA, which normally happens after each round of the peptidyl transfer reaction. In turn, the productive state of A76 of the P-site tRNA could be stabilized by the presence of the peptide, not just a single formyl-methionine residue. To evaluate this possibility, we tested the ability of MADU to interfere with the tripeptide formation *in vitro* using pre-formed elongation complex carrying dipeptidyl-tRNA in the P site (Supplementary Figure S4). MADU exhibited no inhibitory effect on tripeptide formation. This result points to the inability of MADU to bind to an elongation complex due to competition with the peptide already present in the P site of the PTC.

Proper positioning and alignment of the nucleophile in the A site and the carbonyl carbon in the P site is absolutely crucial for the peptide bond formation to occur (24,25). Therefore, inability of the CCA-ends of both the A-site and the P-site tRNA substrates to be properly positioned in the PTC in the presence of MADU explains why type A streptogramins, and MADU in particular, inhibit peptide bond formation. With the exception of the flipped-out A76 for the P-tRNA and distorted CCA-end of the A-tRNA, we can still observe the entire tRNA substrates bound to the A

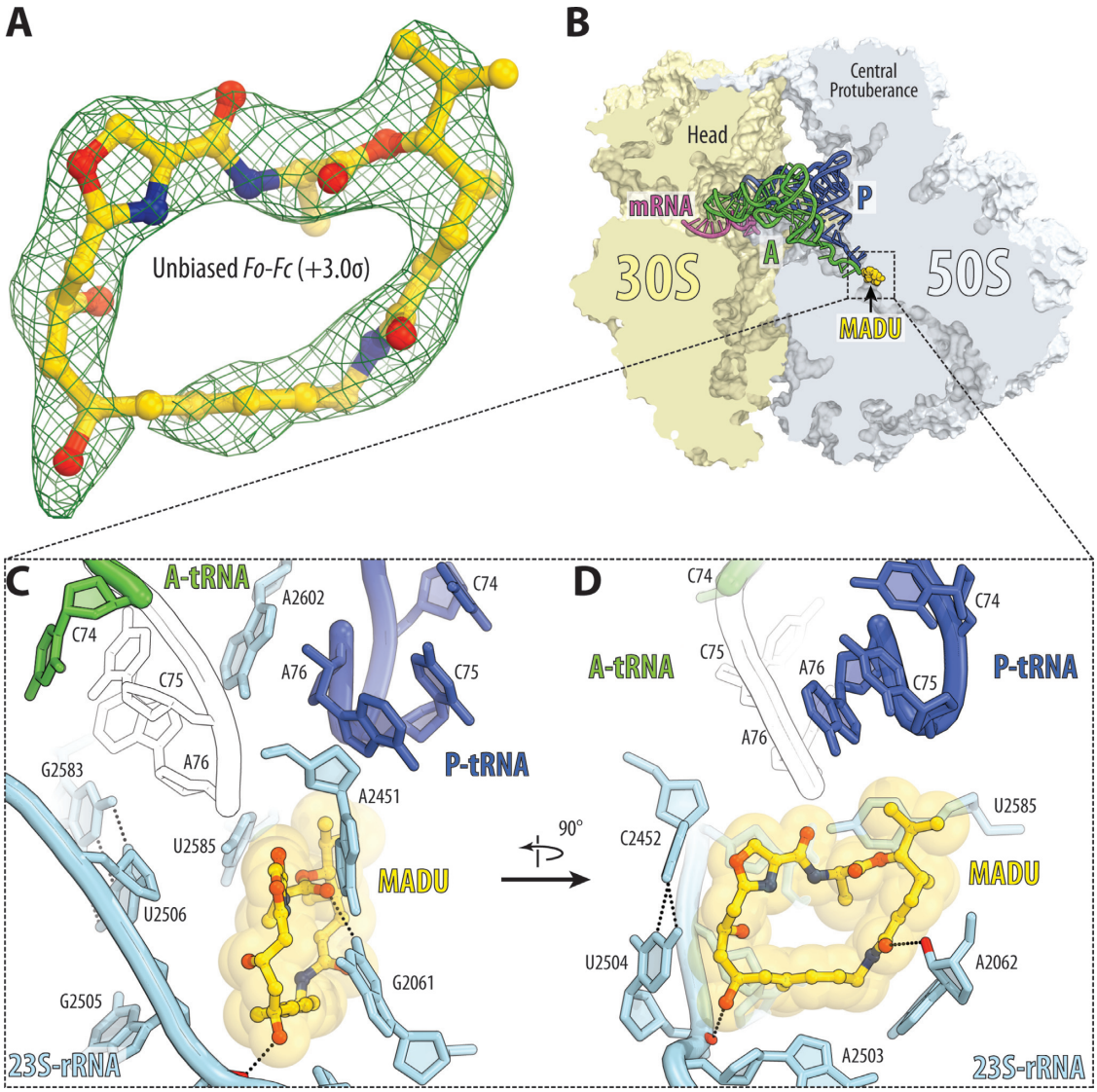

Figure 2. Structures of MADU in complex with the 70S ribosome and A- and P-tRNAs. (**A**) Difference Fourier map of MADU in complex with the *T. thermophilus* 70S ribosome (green mesh). The refined model of MADU (yellow) is displayed in its respective electron density before the refinement. The unbiased ($F_{obs} - F_{calc}$) difference electron density map is contoured at 3σ. Carbon atoms are yellow, nitrogens are blue, and oxygens are red. (**B**) Overview of the MADU binding site (yellow) in the *T. thermophilus* 70S ribosome viewed as a cross-cut through the peptide exit tunnel. The 30S subunit is shown in light yellow, the 50S subunit is in light blue, the mRNA is magenta and the A- and P-site tRNAs are green and dark blue, respectively. The E-site tRNA is omitted for clarity. (**C**, **D**) Close-up views of the MADU binding site shown in panel (B). The *E. coli* nucleotide numbering is used throughout. Nucleotides C75 and A76 of the A-site tRNA are shown as black contour to emphasize that this part of the tRNA is not visible in the electron density upon MADU binding.

and P sites of the ribosome in the presence of MADU. This result suggests that streptogramins A work via a more sophisticated mechanism, than the one suggested previously – binding of tRNAs to the ribosome is not inhibited by MADU, however, their CCA-ends carrying the amino acids cannot be properly oriented to form a peptide bond.

MADU induces conformational rearrangements in the PTC

MADU forms extensive interactions with several conserved nucleotides of the PTC. For instance, the oxazole ring of MADU stacks with A2451 of the 23S rRNA (Figures 2C, and 3D) and a π-stacking interaction is also formed by the C6-amide group with nucleotide A2062 of the 23S rRNA (Figures 2D, and 3C, D). Interestingly, A2062 rotates by ∼90° upon binding of the antibiotic to the ribosome (Figure 3C and D). Similar interactions between other members of the streptogramin A family and vacant ribosomes from *H. marismortui* (4) and *E. coli* (3) have been observed previously.

Upon binding of MADU to the ribosome, nucleotides U2506 and U2585 of the 23S rRNA undergo a significant conformational change (Figure 3C and D). U2506 rotates by >90° away from the bound antibiotic molecule to a location where it forms a wobble base-pair with nucleotide G2583. U2585 moves toward the antibiotic to form a π-stacking interaction with the C1–C2 atoms (Figure

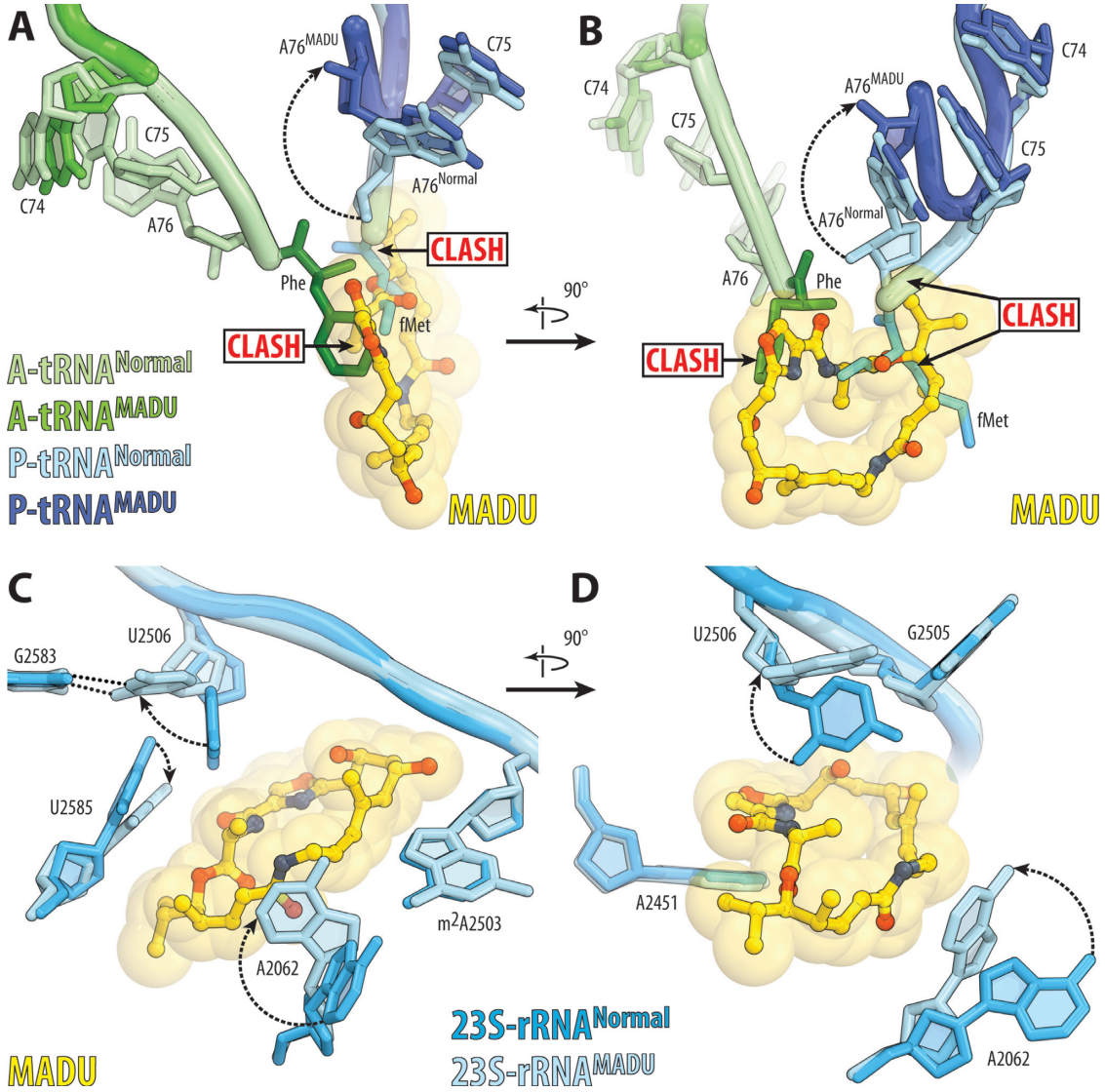

Figure 3. Effects of MADU binding on the conformations of the P-site tRNA and 23S rRNA. (**A**, **B**) Comparison of the positions of the CCA-ends of the A- and P-site tRNAs in the presence of MADU (green and dark blue, respectively) and its absence with the canonical positions of the aminoacylated tRNAs. For reference, the fully accommodated tRNA in the A site (light green with the Phe moiety shown in dark green) and the P-site tRNA (light blue with the fMet moiety colored in blue) are shown from two different views. The structure coordinates for the position of the aminoacylated tRNAs in the pre-attack state are from the PDB entry 1VY4 (24). Note that in the presence of MADU, proper positioning of both A- and P-site substrates is precluded due to the indicated steric clashes. Moreover, A76 of the P-site tRNA flips out by about 180 degrees into a new conformation, in which it no longer forms H-bond interactions with A2451 and the A-site substrate that are required for efficient peptide bond formation. (**C**, **D**) Comparison of the positions of key nucleotides in the 23S rRNA around the PTC in the presence of MADU (light blue) and in the canonical pre-attack state (blue) without the drug, viewed from two different orientations. Several nucleotides in the PTC undergo substantial conformational changes upon MADU binding (shown by dashed arrows). For example, U2506 rotates by more than 90° away from the bound MADU into a location where it forms a wobble base-pair with the nucleotide G2583, while U2585 and A2062 move towards MADU to form π-stacking interactions with the antibiotic.

3C). Interestingly, rearrangements of nucleotides U2506 and U2585 upon streptogramin A binding to the ribosome were suggested before based on chemical foot-printing data (26).

An opposite conformational change has been observed in the *H. marismortui* 50S subunit upon transition from an inactive to an active state of the PTC (Supplementary Figure S5A) (25). It was hypothesized that the disruption of the U2506•G2583 wobble pair leads to the activation of the peptidyl transferase center (25). The formation of U2506•G2583 wobble pair induced by MADU has not been seen before in any of the *T. thermophilus* ribosome structures, suggesting that the PTC of the latter always resides in the active conformation until being forced into the inactive state by binding of MADU (Supplementary Figure S5B). Curiously, formation of the same wobble pair was not observed in the *E. coli* ribosome complexes with several streptogramin A antibiotics, which might be due to the absence of tRNAs in those structures (3). However, in the *E. coli* ribosome structures with proline-containing streptogramins A, U2585 is positioned differently than that in the current structure with the alanine-containing MADU.

We reasoned that this is likely due to the fact that the bulkier proline residue collides with U2585 and causes its movement away from the inhibitor, while the smaller alanine residue of MADU interacts with U2585 favoring its movement towards the antibiotic. This result exemplifies how subtle differences in the structure of an antibiotic can result in distinct and even opposite conformational rearrangements of the target macromolecular complex.

Structural bases for the resistance mechanisms against MADU.

Resistance to many peptidyl transferase inhibitors (including streptogramins A) can be conferred by Cfr, a methyltransferase that monomethylates the C8 position of A2503 of the 23S rRNA (27). Modelling the C8-methylation of A2503 shows a collision with the ribosome-bound MADU, suggesting that Cfr-mediated MADU resistance is likely to exist (Supplementary Figure S6A). Likewise, mutation A2503G (26) that confers resistance to chloramphenicol and streptogramin A antibiotics is likely to shift this nucleotide into a new position, in which it may interfere with the antibiotic binding site and lead to resistance. An alternative mechanism of resistance to MADU and other streptogramin A antibiotics is acetylation of the C12-hydroxyl by the VatB acetyltransferase that renders the drug inactive (Supplementary Figure S6B) (28). *In silico* modelling of the acetyl group onto the C12-hydroxyl of MADU shows a steric clash with the phosphate group between U2504 and G2505 of the 23S rRNA, providing a structural basis for the poor antimicrobial activity of acetylated compounds (Supplementary Figure S6C). A similar conclusion has previously been made based on the structure of the *E. coli* ribosome with other streptogramin A antibiotics (3).

CONCLUSIONS

We have characterized the mode of interaction of the PTC inhibitor MADU, an alanine-containing streptogramin A antibiotic, with the ribosome. Our study provides insights into the mechanism of action of this class of inhibitors. MADU inhibits the bacterial ribosome prior to the formation of the first peptide bond by preventing the proper positioning of both A- and P-site tRNA substrates making peptide bond formation impossible. We also described a previously unseen drug-induced rearrangement of nucleotides U2506 and U2585 of the 23S rRNA resulting in the formation of the U2506•G2583 wobble pair that is attributed to a catalytically inactive state of the PTC. These data expand our knowledge of the mechanisms by which peptidyl transferase inhibitors modulate the catalytic activity of the ribosome. The potency of MADU as a ribosome inhibitor makes it an attractive compound for further development by medicinal chemists, and we expect that the structure of the MADU-ribosome complex described here will serve as a scaffold to such studies.

ACCESSION NUMBERS

Coordinates and structure factors were deposited in the RCSB Protein Data Bank with accession codes 5VP2 for the *Tth* 70S ribosome in complex with madumycin II, mRNA, A-, P- and E-site tRNAs.

SUPPLEMENTARY DATA

Supplementary Data are available at NAR Online.

ACKNOWLEDGEMENTS

We thank all members of the P.V.S., A.L.K. and Y.S.P. laboratories for discussions and critical feedback. We thank Dr Matthieu Gagnon and Nikolay Aleksashin for critical reading of the manuscript. We thank staff at NE-CAT beamline 24ID-C for help with data collection and freezing of the crystals, especially Drs Kanagalakhatta Rajashankar, Malcolm Capel, Frank Murphy, Igor Kourinov, Anthony Lynch, Surajit Banerjee, David Neau, Jonathan Schuermann, Narayanasami Sukumar, James Withrow, Kay Perry and Cyndi Salbego.

FUNDING

Illinois State startup funds [to Y.S.P.]; Russian Foundation for Basic Research [16-04-01100 to P.V.S., 15-34-20139 to I.A.O.]; Russian Science Foundation [15-14-00006 to P.V.S.]; Moscow University Development Program [PNR 5.13 to P.V.S.]. This work is based upon research conducted at the Northeastern Collaborative Access Team beamlines, which are funded by the National Institute of General Medical Sciences from the National Institutes of Health [P41 GM103403 to NE-CAT]. The Pilatus 6M detector on 24ID-C beam line is funded by a NIH-ORIP HEI [S10 RR029205 to NE-CAT]. This research used resources of the Advanced Photon Source, a U.S. Department of Energy (DOE) Office of Science User Facility operated for the DOE Office of Science by Argonne National Laboratory [DE-AC02-06CH11357]. Funding for open access charge: Illinois State startup funds.
Conflict of interest statement. None declared.

REFERENCES

1. Wilson,D.N. (2014) Ribosome-targeting antibiotics and mechanisms of bacterial resistance. *Nat. Rev. Microbiol.*, **12**, 35–48.
2. Johnston,N.J., Mukhtar,T.A. and Wright,G.D. (2002) Streptogramin antibiotics: mode of action and resistance. *Curr. Drug Targets*, **3**, 335–344.
3. Noeske,J., Huang,J., Olivier,N.B., Giacobbe,R.A., Zambrowski,M. and Cate,J.H. (2014) Synergy of streptogramin antibiotics occurs independently of their effects on translation. *Antimicrob. Agents Chemother.*, **58**, 5269–5279.
4. Hansen,J.L., Moore,P.B. and Steitz,T.A. (2003) Structures of five antibiotics bound at the peptidyl transferase center of the large ribosomal subunit. *J. Mol. Biol.*, **330**, 1061–1075.
5. Harms,J.M., Schlunzen,F., Fucini,P., Bartels,H. and Yonath,A. (2004) Alterations at the peptidyl transferase centre of the ribosome induced by the synergistic action of the streptogramins dalfopristin and quinupristin. *BMC Biol.*, **2**, 4.
6. Brazhnikova,M.G., Kudinova,M.K., Potapova,N.P., Filippova,T.M., Borowski,E., Zielinskii,Y. and Golic,J. (1975) Structure of the antibiotic madumycin. *Bioorg. Khim.*, **1**, 1383–1384.
7. Chamberlin,J.W. and Chen,S. (1977) A2315, new antibiotics produced by Actinoplanes philippinensis. Structure of A2315A. *J. Antibiot. (Tokyo)*, **30**, 197–201.

8. Polikanov,Y.S., Osterman,I.A., Szal,T., Tashlitsky,V.N., Serebryakova,M.V., Kusochek,P., Bulkley,D., Malanicheva,I.A., Efimenko,T.A., Efremenkova,O.V. *et al.* (2014) Amicoumacin A inhibits translation by stabilizing mRNA interaction with the ribosome. *Mol. Cell*, **56**, 531–540.
9. Svetlov,M.S., Kommer,A., Kolb,V.A. and Spirin,A.S. (2006) Effective cotranslational folding of firefly luciferase without chaperones of the Hsp70 family. *Protein Sci.*, **15**, 242–247.
10. Konevega,A.L., Soboleva,N.G., Makhno,V.I., Semenkov,Y.P., Wintermeyer,W., Rodnina,M.V. and Katunin,V.I. (2004) Purine bases at position 37 of tRNA stabilize codon-anticodon interaction in the ribosomal A site by stacking and Mg2+-dependent interactions. *RNA*, **10**, 90–101.
11. Bruell,C.M., Eichholz,C., Kubarenko,A., Post,V., Katunin,V.I., Hobbie,S.N., Rodnina,M.V. and Bottger,E.C. (2008) Conservation of bacterial protein synthesis machinery: initiation and elongation in Mycobacterium smegmatis. *Biochemistry*, **47**, 8828–8839.
12. Orelle,C., Szal,T., Klepacki,D., Shaw,K.J., Vazquez-Laslop,N. and Mankin,A.S. (2013) Identifying the targets of aminoacyl-tRNA synthetase inhibitors by primer extension inhibition. *Nucleic Acids Res.*, **41**, e144.
13. Orelle,C., Carlson,S., Kaushal,B., Almutairi,M.M., Liu,H., Ochabowicz,A., Quan,S., Pham,V.C., Squires,C.L., Murphy,B.T. *et al.* (2013) Tools for characterizing bacterial protein synthesis inhibitors. *Antimicrob. Agents Chemother.*, **57**, 5994–6004.
14. Polikanov,Y.S., Starosta,A.L., Juette,M.F., Altman,R.B., Terry,D.S., Lu,W., Burnett,B.J., Dinos,G., Reynolds,K.A., Blanchard,S.C. *et al.* (2015) Distinct tRNA accommodation intermediates observed on the ribosome with the antibiotics hygromycin A and A201A. *Mol. Cell*, **58**, 832–844.
15. Polikanov,Y.S., Melnikov,S.V., Soll,D. and Steitz,T.A. (2015) Structural insights into the role of rRNA modifications in protein synthesis and ribosome assembly. *Nat. Struct. Mol. Biol.*, **22**, 342–344.
16. Polikanov,Y.S., Blaha,G.M. and Steitz,T.A. (2012) How hibernation factors RMF, HPF, and YfiA turn off protein synthesis. *Science*, **336**, 915–918.
17. McCoy,A.J., Grosse-Kunstleve,R.W., Adams,P.D., Winn,M.D., Storoni,L.C. and Read,R.J. (2007) Phaser crystallographic software. *J. Appl. Crystallogr.*, **40**, 658–674.
18. Emsley,P. and Cowtan,K. (2004) Coot: model-building tools for molecular graphics. *Acta Crystallogr. D Biol. Crystallogr.*, **60**, 2126–2132.
19. Adams,P.D., Afonine,P.V., Bunkoczi,G., Chen,V.B., Davis,I.W., Echols,N., Headd,J.J., Hung,L.W., Kapral,G.J., Grosse-Kunstleve,R.W. *et al.* (2010) PHENIX: a comprehensive Python-based system for macromolecular structure solution. *Acta Crystallogr. D Biol. Crystallogr.*, **66**, 213–221.
20. Chinali,G., Moureau,P. and Cocito,C.G. (1984) The action of virginiamycin M on the acceptor, donor, and catalytic sites of peptidyltransferase. *J. Biol. Chem.*, **259**, 9563–9568.
21. Hartz,D., McPheeters,D.S., Traut,R. and Gold,L. (1988) Extension inhibition analysis of translation initiation complexes. *Methods Enzymol.*, **164**, 419–425.
22. Kirillov,S.V., Porse,B.T. and Garrett,R.A. (1999) Peptidyl transferase antibiotics perturb the relative positioning of the 3′-terminal adenosine of P/P'-site-bound tRNA and 23S rRNA in the ribosome. *RNA*, **5**, 1003–1013.
23. Rozov,A., Westhof,E., Yusupov,M. and Yusupova,G. (2016) The ribosome prohibits the G*U wobble geometry at the first position of the codon-anticodon helix. *Nucleic Acids Res.*, **44**, 6434–6441.
24. Polikanov,Y.S., Steitz,T.A. and Innis,C.A. (2014) A proton wire to couple aminoacyl-tRNA accommodation and peptide-bond formation on the ribosome. *Nat. Struct. Mol. Biol.*, **21**, 787–793.
25. Schmeing,T.M., Huang,K.S., Strobel,S.A. and Steitz,T.A. (2005) An induced-fit mechanism to promote peptide bond formation and exclude hydrolysis of peptidyl-tRNA. *Nature*, **438**, 520–524.
26. Porse,B.T. and Garrett,R.A. (1999) Sites of interaction of streptogramin A and B antibiotics in the peptidyl transferase loop of 23 S rRNA and the synergism of their inhibitory mechanisms. *J. Mol. Biol.*, **286**, 375–387.
27. Long,K.S., Poehlsgaard,J., Kehrenberg,C., Schwarz,S. and Vester,B. (2006) The Cfr rRNA methyltransferase confers resistance to Phenicols, Lincosamides, Oxazolidinones, Pleuromutilins, and Streptogramin A antibiotics. *Antimicrob. Agents Chemother.*, **50**, 2500–2505.
28. Allignet,J. and el Solh,N. (1995) Diversity among the Gram-positive acetyltransferases inactivating streptogramin A and structurally related compounds and characterization of a new staphylococcal determinant, vatB. *Antimicrob. Agents Chemother.*, **39**, 2027–2036.